



Published in final edited form as:

*Nat Neurosci.* 2015 October ; 18(10): 1483–1492. doi:10.1038/nn.4090.

## Coordinated forms of noradrenergic plasticity in the locus coeruleus and primary auditory cortex

Ana Raquel O. Martins<sup>1,2,3,4,5,6,7</sup> and Robert C. Froemke<sup>1,2,3,4,5,\*</sup>

<sup>1</sup>Skirball Institute for Biomolecular Medicine, New York University School of Medicine, New York, NY, 10016 USA

<sup>2</sup>Neuroscience Institute, New York University School of Medicine, New York, NY, 10016 USA

<sup>3</sup>Department of Otolaryngology, New York University School of Medicine, New York, NY, 10016 USA

<sup>4</sup>Department of Neuroscience and Physiology, New York University School of Medicine, New York, NY, 10016 USA

<sup>5</sup>Center for Neural Science, New York University, New York, NY, 10003 USA

<sup>6</sup>PhD Programme in Experimental Biology and Biomedicine, University of Coimbra, Portugal

<sup>7</sup>Center for Neurosciences and Cell Biology, University of Coimbra, Portugal

### Abstract

The cerebral cortex is plastic and represents the world according to the significance of sensory stimuli. However, cortical networks are embodied within complex circuits including neuromodulatory systems such as the noradrenergic locus coeruleus, providing information about internal state and behavioral relevance. While norepinephrine is important for cortical plasticity, it is unknown how modulatory neurons themselves respond to changes of sensory input. Here we examine how locus coeruleus neurons are modified by experience, and the consequences of locus coeruleus plasticity on cortical representations and sensory perception. We made whole-cell recordings from rat locus coeruleus and primary auditory cortex (AI), pairing sounds with locus coeruleus activation. Although initially unresponsive, locus coeruleus neurons developed and maintained auditory responses afterwards. Locus coeruleus plasticity induced changes in AI responses lasting at least hours and improved auditory perception for days to weeks. Our results demonstrate that locus coeruleus is highly plastic, leading to substantial changes in regulation of brain state by norepinephrine.

---

The central nervous system can be modified by experience and maintains the capacity for functional reorganization throughout life<sup>1–6</sup>. This plasticity is a major feature of AI, especially for forming representations of behaviorally-significant sensory signals such as

---

Reprints and permissions information is available at [www.nature.com/reprints](http://www.nature.com/reprints).

\*To whom correspondence should be addressed: Phone: 212-263-4082, [robert.froemke@med.nyu.edu](mailto:robert.froemke@med.nyu.edu).

**Author contributions:** A.R.O.M. performed the experiments. A.R.O.M. and R.C.F. analyzed the experiments and wrote the paper.

The authors declare that they have no competing financial interests.

speech, music and other forms of acoustic communication<sup>7–12</sup>. Changes in neural circuits and behavior can be incredibly long-lasting, particularly after arousing or stressful events, but the processes and mechanisms by which cortical networks are modified and affect sensory perception are unclear.

Long-term cortical plasticity requires both sensory experience and activation of neuromodulatory systems, which relay behavioral context to local cortical circuits<sup>13–19</sup>. Among these neuromodulators, norepinephrine is important for learning, synaptic plasticity, and modification of sensory representations<sup>20–25</sup>, and is released throughout the brain by locus coeruleus neurons during periods of arousal, anxiety, and stress<sup>26–29</sup>. Locus coeruleus neurons are activated by noxious and surprising stimuli, and also respond directly to previously-innocuous stimuli that have been linked to behaviorally-significant episodes in the past<sup>30–33</sup>. It is hypothesized that locus coeruleus plays a major role in adjusting the gains of cortical synapses in a task-dependent manner; in particular, higher-frequency phasic activity of noradrenergic neurons may facilitate the formation of task-specific behavioral patterns, to optimize perceptual abilities and motor outputs<sup>26</sup>. However, it is unknown how locus coeruleus neurons are affected by experience, or how modifications to noradrenergic and cortical circuits interact and are coordinated. Here we directly examine the relationship between locus coeruleus activity and cortical plasticity enabled by norepinephrine, by recording from adult rat locus coeruleus and AI neurons in parallel with behavioral experiments on auditory perception, to reveal synaptic mechanisms and network dynamics involved in perceptual learning under noradrenergic control.

## Results

### Locus coeruleus plasticity

To determine how locus coeruleus is altered by experience, we first asked how locus coeruleus neurons respond to sensory stimuli. We recorded from these neurons in anesthetized adult rats (Fig. 1, Supplementary Figs. 1, 2), and locus coeruleus was identified by response to tail pinch and anatomical identification of electrode position. Intense stimulation (foot shock) produced phasic, high-frequency spiking (Supplementary Fig. 1a), while innocuous stimuli (pure tones) did not evoke detectable responses (Supplementary Fig. 1b, 'Pre'). However, after tones were repetitively paired with foot shock for 1–5 minutes, paired tones could evoke locus coeruleus spikes for 1+ hours (Supplementary Fig. 1b, 'Post'). Spontaneous activity and responses to foot shock were qualitatively similar under both ketamine and pentobarbital anesthesia (Supplementary Fig. 2), although there was a trend for firing rates to be reduced in the presence of ketamine.

We then examined if pairing auditory stimuli with locus coeruleus activity ('locus coeruleus pairing') was sufficient to modify neuronal responses. Pairing was performed either by depolarization through the recording electrode or extracellular stimulation. For single-cell depolarization, we made current-clamp recordings from locus coeruleus neurons, and measured responses to pure tones (0.5–32 kHz) 5–20 minutes before and 5+ minutes after pairing postsynaptic spike with a pure tone of a specific frequency at 70 dB sound pressure level (SPL). After the baseline period, neurons were phasically depolarized at 20 Hz for 500 msec, repeated at 0.5–1 Hz for 1–5 minutes (Fig. 1b), similar to firing patterns observed in

locus coeruleus neurons during foot shock (Supplementary Fig. 1a). This procedure mimics what can occur when sounds are linked to arousing situations<sup>29,33</sup>, although in some cases locus coeruleus neurons can fire at higher rates and in shorter bursts<sup>34</sup>. Electrode positions were confirmed by measuring responses to tail pinch (Supplementary Fig. 1a) and post hoc histology (Supplementary Fig. 1c, e), with some locus coeruleus neurons filled with biocytin through the whole-cell pipette and co-labeled with an antibody to tyrosine hydroxylase (TH).

Pairing tones with single-cell depolarization induced responses to auditory stimuli in previously-unresponsive locus coeruleus neurons that lasted for the duration of the recordings. An example in vivo whole-cell recording is shown in Figure 1c. Initially, this cell did not respond to sounds. However, after pairing 16 kHz tones with postsynaptic spiking, 16 kHz tones evoked sizable EPSPs at ~30 msec latency, and tone-evoked responses lasted for the recording duration. Locus coeruleus plasticity required NMDA receptors, as local infusion of AP5 (1 mM) prevented emergence of tone-evoked responses after pairing (Fig. 1d). These results are reminiscent of ‘silent synapses’ activated after induction of long-term potentiation, although here it appeared that auditory responses had developed in formerly ‘silent cells’.

We tested how long these auditory responses would last after pairing. To simultaneously induce plasticity in multiple locus coeruleus neurons, we paired pure tones with extracellular locus coeruleus stimulation (20 Hz for 500 msec at 0.5–1 Hz, 1–5 minutes). We confirmed that stimulation was confined to a small area (<500  $\mu\text{m}$ ) around the electrode (Supplementary Fig. 1f). We made current-clamp and cell-attached recordings in vivo; after the first recording, 0–4 more recordings were obtained from different neurons in the same animal, to assess degree and duration of changes to other locus coeruleus neurons after a single pairing episode.

Three recordings from the same animal are shown in Figure 1e, a current-clamp recording before and after pairing (Fig. 1e, left; gray, red), a cell-attached recording 5+ hours after pairing (Fig. 1e, right), and a final current-clamp recording 6+ hours afterward (Fig. 1e, left; black). The paired tone was 16 kHz at 70 dB SPL. Locus coeruleus cells continued to respond to paired tones for hours after pairing. Additionally, locus coeruleus plasticity could be specific to paired tones, as responses to unpaired tones were sometimes initially enhanced but not persistently modified after pairing (Fig. 1e, left).

The duration of locus coeruleus plasticity as measured by z-scores is shown in Figure 1f, with non-normalized values of synaptic and spiking responses shown in Supplementary Figure 3. Significant increases in synaptic strength and spike generation (Fig. 1f) lasted for at least several hours after pairing, unless locus coeruleus plasticity was prevented with AP5. These findings demonstrate that locus coeruleus neurons can become part of the overall circuit activated by once-innocuous stimuli. Importantly, this might lead to noradrenergic modulation of target projection areas in response to tonal presentation alone. Therefore we focused the rest of our experiments on the functional consequences of neuromodulatory plasticity on cortical responses and perceptual learning.

## Locus coeruleus pairing modifies AI responses

A major output of locus coeruleus is the cerebral cortex, where noradrenergic modulation plays a key role in sensory processing and control of behavior<sup>26–28</sup>. To determine how noradrenergic modulation affected cortical sensory representations, we made in vivo recordings from AI neurons and monitored tone-evoked responses before and after pairing (Figs. 2, 3, Supplementary Fig. 4). We made whole-cell recordings from 91 AI cells (51 current-clamp, 40 voltage-clamp) and 50 cell-attached recordings in 49 adult rats implanted with stimulation electrodes in locus coeruleus (Fig. 2a), as well as 25 AI cells (13 current-clamp and 12 cell-attached) from five adult *TH-Cre* rats expressing channelrhodopsin-2 specifically in TH-positive locus coeruleus neurons (Fig. 3a). Baseline responses to pure tones were recorded from AI neurons, locus coeruleus pairing was performed, and responses measured as long as recordings remained stable. When the first recording ended, we sequentially made 1–7 more recordings from that cortical location to document the dynamics of post-pairing response modification over 12 hours. We quantified changes to tuning curves over multiple cells by measuring relative shift in best frequency from the original best frequency towards the paired frequency (e.g., 100% shift indicates that best frequency became the paired frequency), and by fitting Gaussians and quantifying increase in tuning curve width measured in standard deviations (e.g., 200% width indicates that standard deviation doubled).

One set of recordings demonstrating the cortical effects of locus coeruleus pairing with electrical stimulation is shown in Figure 2b, c. We recorded from five neurons from the same region of AI initially tuned to 4 kHz, for 11 hours after pairing. The first cell recorded in current-clamp had a best frequency of 4 kHz (Fig. 2c, upper left, gray). The paired frequency was 16 kHz at 70 dB SPL; after pairing, responses to all tones increased (Fig. 2b) across the tuning curve and the best frequency shifted to the paired frequency (Fig. 2c, upper left, black). We measured cell-attached spiking responses 50 minutes after pairing in this cell; 16 kHz remained the best frequency (Fig. 2c, upper right). Over the next ten hours, we obtained four more recordings (two current-clamp, two cell-attached; Fig. 2c middle, bottom). Tuning width recovered but 16 kHz remained the best frequency.

We also examined the effects of optical stimulation in *TH-Cre* rats expressing the ‘ChETA’ variant of channelrhodopsin-2 in locus coeruleus neurons via stereotaxic injection of Cre-dependent adeno-associated virus (pAAV5-Ef1a-DIO-ChETA-EYFP). These *TH-Cre* animals had optical fibers implanted in locus coeruleus for stimulation specifically of the noradrenergic neurons during pairing (Fig. 3a). One set of recordings from the same animal is shown in Figure 3b. Before pairing the best frequency was 1 kHz and responses were weak. After pairing, responses increased and tuning shifted to the paired 16 kHz frequency up to 7.5 hours afterwards for both synaptic and spiking responses. Thus electrical stimulation and optogenetic stimulation of the locus coeruleus both affect AI receptive fields, increasing responses to auditory stimuli and at least initially reducing the tuning width of cortical neurons. Pairing with electrical vs. optogenetic stimulation share some features, but there may be some differences in outcomes, reflecting activation of overlapping but distinct cell populations with one method compared to the other.

Overall, three general features of cortical plasticity induced by locus coeruleus pairing were apparent: 1) large increases in tone-evoked responses to all stimuli; 2) shifts in best frequency towards paired inputs; and 3) return of average tuning width over several hours, with maintained preference at the paired input for the duration of the recordings (Fig. 4, Supplementary Fig. 4). In individual neurons, responses at paired inputs were substantially larger 5–10 minutes after pairing as well as 45–60 minutes after pairing (Fig. 4a). Responses to unpaired inputs were also enhanced 5–10 minutes after pairing, but returned towards original levels 45–60 minutes post-pairing (Fig. 4b). Similar enhancements also occurred for AI intensity tuning (Supplementary Fig. 5), leading to stronger responses overall, albeit with increased preference around paired levels.

As a consequence, paired inputs tended to become the best input within minutes after pairing, shifting best frequency and broadening tuning. Surprisingly, this shift in tuning could last 7–12 hours (Fig. 4c, Supplementary Fig. 4a), whereas tuning width recovered and was statistically similar to baseline tuning widths within 3–4 hours (Fig. 4d). These changes were also observed for spiking responses in current-clamp and cell-attached recordings (Fig. 4e, f, Supplementary Fig. 4b) as well as multiunit recordings (Supplementary Fig. 6). Similar modifications could be induced under pentobarbital anesthesia (, Supplementary Figure 7).

These effects are qualitatively different from the consequences of nucleus basalis pairing<sup>17,35</sup>, which instead induces stimulus-specific and shorter-lasting changes in AI frequency tuning (Supplementary Fig. 8). Although the locus coeruleus and nucleus basalis modulatory systems are intimately related<sup>20,32</sup>, the effects of locus coeruleus pairing on AI responses seemed independent of cholinergic modulation as they were not affected by cortical application of the muscarinic acetylcholine receptor antagonist atropine (Supplementary Fig. 9).

Thus the main effect of locus coeruleus pairing on cortical responses is to first greatly increase responses to all sensory stimuli, regardless of context, before retaining an enduring specificity for paired inputs. In the remainder of this study, we investigate the circuit mechanisms of cortical plasticity (Fig. 5, Supplementary Figs. 10, 11), the relation between locus coeruleus plasticity and AI plasticity (Fig. 6, 7), and the perceptual consequences from these modifications to auditory representations (Fig. 8, Supplementary Fig. 12).

### Cortical circuit effects of locus coeruleus pairing

We found that locus coeruleus pairing could induce tone-evoked responses in previously-silent AI cells (Fig. 5a), as well as convert subthreshold (non-spiking) responses into suprathreshold (spiking) responses (Fig. 5b). Pairing increased the average size of paired EPSCs and EPSPs (Fig. 5c). Interestingly, tone-evoked responses were not detected in 9/37 AI neurons before pairing. In 6/9 of these non-responsive cells, pairing rapidly induced significant responses that were maintained for the recording duration. Of the other 28 cells, 20/28 neurons showed increased responses while in 8/28 neurons the tone-evoked synaptic response was reduced after pairing.

We next measured changes to tone-evoked spiking. Pairing greatly increased spike output by AI neurons, measured in current-clamp and cell-attached recordings (Fig. 5d). Paired tones initially evoked spikes only in 3/21 current-clamp and 9/12 cell-attached recordings. After pairing, spikes were evoked in 13/21 current-clamp and 12/12 cell-attached recordings (in 2/33 recordings, spiking was reduced after pairing).

The neuromodulator acetylcholine reduces evoked inhibition to shift cortical excitatory-inhibitory balance in favor of excitation<sup>17</sup>. Thus we next asked if noradrenergic modulation via locus coeruleus stimulation had a similar effect, using in vivo voltage-clamp recordings from AI neurons to assess changes to inhibitory postsynaptic currents (IPSCs). We found that locus coeruleus pairing greatly increased tone-evoked EPSCs and IPSCs together (Supplementary Fig. 10). However, pairing decreased spontaneous inhibition for several minutes during and after pairing. This was primarily expressed as a reduction in spontaneous IPSC rate (Fig. 5e, left), while spontaneous IPSC amplitudes (Fig. 5e, right) and the rates and amplitude of spontaneous EPSCs (Fig. 5f) were unaffected.

These findings show that locus coeruleus activation seems to specifically decrease tonic (spontaneous) inhibition rather than phasic (stimulus-evoked) inhibition. This provides a basic gain control mechanism by which responses to any incoming stimuli would be transiently enhanced after noradrenergic modulation, as a reduction in spontaneous inhibition would affect all subsequent inputs, paired and unpaired. In this manner, locus coeruleus may provide a broadband signal for increasing sensory processing in novel or hazardous environments, where possibly one or more of many environmental cues are important for behavioral performance. Furthermore, these results also suggest that the sources of spontaneous and tone-evoked inhibition are under distinct forms of neuromodulatory control.

We asked if reducing overall inhibitory tone could lead to similar changes in tone-evoked synaptic responses and frequency tuning. We performed pharmacological experiments to reduce GABAergic inhibition (Supplementary Fig. 11), either by bicuculline iontophoresis or intracellular perfusion with picrotoxin. We made voltage-clamp recordings to measure synaptic frequency tuning, then presented tones of a given frequency during five minutes of bicuculline iontophoresis. Ten minutes after iontophoresis was over, we observed an enduring enhancement of tone-evoked excitatory and inhibitory responses together (Supplementary Fig. 11a). In other experiments, GABAergic inhibition was constitutively blocked by including picrotoxin in the whole-cell pipette. Because this disinhibition alone leads to a substantial enhancement of excitatory responses, we waited 10 minutes for dialysis of picrotoxin through the recording pipette before starting tonal stimulation. We monitored responses to a single tone frequency, and observed a progressive strengthening of these synaptic responses, in an activity-dependent manner that required NMDA receptors (Supplementary Fig. 11b). Thus tonic disinhibition can be an effective mechanism for enhancing synaptic responses in a long-lasting manner.

### **Locus coeruleus plasticity controls cortical plasticity**

We next performed a series of pharmacological studies to understand the mechanistic basis of AI changes induced by locus coeruleus pairing, and connect these forms of subcortical

and cortical plasticity. Surprisingly, we found that locus coeruleus plasticity was both sufficient (Fig. 6) and necessary (Fig. 7) for the induction and maintenance of cortical plasticity.

First, we paired tones with norepinephrine iontophoresis locally in AI instead of locus coeruleus stimulation (Fig. 6a). While ‘norepinephrine pairing’ increased responses and shifted best frequency towards the paired input, these changes were temporary and lasted less than an hour. Cortical norepinephrine, paired with sensory input, is not by itself sufficient for the long-lasting changes to AI responses observed with locus coeruleus pairing.

We then examined whether noradrenergic receptor activation was at all required for the effects of locus coeruleus pairing. Topical application of the alpha-adrenergic receptor antagonist phentolamine immediately prior to pairing initially blocked effects of pairing. However, minutes after pairing ended and phentolamine was no longer applied, AI tuning curves shifted towards the paired frequency, resulting in enduring changes similar to those induced by locus coeruleus pairing (Fig. 6b).

Instead, noradrenergic receptor activation in AI was required hours after locus coeruleus pairing had ended. To assess the requirement for neuromodulation after pairing, phentolamine was topically applied to AI continuously over the duration of the experiment starting ~30 minutes post-pairing. Although locus coeruleus pairing initially produced substantial shifts in tuning curves, tens of minutes later these changes were diminished and AI tuning curves shifted back to their original best frequency in the presence of phentolamine (Fig. 6c).

These findings reveal two important features of locus coeruleus pairing and neuromodulatory plasticity. First, that alpha-noradrenergic receptor activation is required for long-lasting expression of changes to cortical sensory representations in response to locus coeruleus pairing. Second, this modulatory control over cortical plasticity must occur within AI itself, because local AI application of noradrenergic receptor antagonist prevented tuning curve shifts. These results then suggest that plasticity of locus coeruleus directly controls AI plasticity. In this scenario, each time paired tones are presented after pairing, newly-responsive locus coeruleus neurons release norepinephrine into AI, maintaining changes to cortical representations in a selective and powerful manner.

Therefore, we asked whether modifications to locus coeruleus neurons were required for cortical plasticity. We recorded from AI neurons before and after locus coeruleus pairing, and used cannulas to infuse AP5 into locus coeruleus to prevent locus coeruleus plasticity. Infusing AP5 into locus coeruleus during pairing reduced the duration of AI modifications. Three cells recorded over eight hours from a 4 kHz region of AI are shown in Figure 7a. The first current-clamp recording showed that 4 kHz was the best frequency (Fig. 7a, left, gray). Locus coeruleus stimulation was paired with 1 kHz tones at 70 dB SPL. Three hours after pairing, a second AI neuron had new preference for 1 kHz (Fig. 7a, right). But eight hours after pairing, tuning reverted to 4 kHz (Fig. 7a, left, black). We conclude that locus

coeruleus plasticity is required for maintenance of AI plasticity over hours, as AP5 infused into locus coeruleus dramatically reduced the duration of AI tuning curve shifts (Fig. 7b).

### Locus coeruleus pairing improves auditory perception

Finally, we asked how these changes to auditory representations induced by locus coeruleus pairing might affect auditory perception. We used a behavioral task involving auditory perceptual learning in adult rats sensitive to plasticity of AI tuning curves<sup>35</sup>. We examined three predictions suggested by our physiological results: 1) behaviorally-important stimuli should be easier to detect and recognize after locus coeruleus pairing, as AI synaptic and spiking responses to tones of all intensities are greatly enhanced; 2) recognition of specific stimuli may initially be impaired, as AI tuning curves first widen and responses to distinct stimuli become more similar for a few hours after locus coeruleus pairing; and 3) improvements to perceptual abilities should persist for hours or perhaps indefinitely even after a single brief pairing episode, given the prolonged maintenance of AI plasticity by locus coeruleus plasticity.

We operantly conditioned 79 adult rats to nose-poke for a food reward in response to 4 kHz target stimuli of any intensity, while withholding responses to six foil tones of other frequencies (Supplementary Fig. 12a). Twenty-two Sprague-Dawley rats were implanted with stimulation electrodes and drug delivery cannulas into locus coeruleus. Nine other animals were *TH-Cre* rats expressing ChETA in locus coeruleus with optical fibers implanted for optogenetic stimulation. We examined perceptual abilities to detect target stimuli over a range of intensities and recognize target stimuli from non-target foils, assessing performance over several days before and after pairing. In other animals we examined whether locus coeruleus pairing would affect the learning rate on a reversal learning task.

First we examined detection abilities. Baseline psychophysical performance of a representative animal is shown in Figure 8a (black). At 50 dB SPL, this animal had near-perfect performance detecting target 4 kHz tones ('Hits', circles) and a low number of responses to foils ('F+', triangles). However, this animal had a low response rate for tones of 20–40 dB SPL. After measuring behavioral responses for 30–60 minutes, we paired 4 kHz tones at 30 dB SPL with locus coeruleus stimulation for 3 minutes while the animal was awake. We then re-tested detection abilities 12 hours later and found that detection at 20–40 dB SPL was greatly enhanced (Fig. 8a, red). Similar improvements in detection were observed for 21 animals, including five *TH-Cre* rats in which optogenetic locus coeruleus pairing was performed (Fig. 8b, c). Remarkably, enhancements of detection abilities lasted up to four and in some cases 20+ days post-pairing (Fig. 8d). Behavioral changes were prevented when AP5 (1 mM) was infused into locus coeruleus before pairing (Fig. 8c, open circles), indicating that locus coeruleus plasticity is required for behavioral improvement. Thus locus coeruleus stimulation facilitates detection of previously-imperceptible stimuli, and brief episodes of pairing optimize signal processing and formation of sensorimotor associations in a circuit distributed throughout cortex and brainstem.

We then asked how pairing would affect abilities to distinguish targets from foils. Initially, foil stimuli were spectrally dissimilar from the target stimulus of 4 kHz, separated at one



octave intervals at 70 dB SPL. Animals easily responded to targets and withheld responses to foils on this ‘wideband’ task before pairing. We then made this task more challenging, by compressing the spectral range of foils from six to one octave, such that foils were similar to the target. Before pairing, behavioral performance on this ‘narrowband’ task was low (Supplementary Fig. 12b), and pairing initially reduced these modest recognition abilities even further for a few hours (Supplementary Fig. 12b, c). However, performance gradually improved, and were improved above baseline levels 12 hours post-pairing (Supplementary Fig. 12d). These changes in auditory perception seem similar to AI modifications observed electrophysiologically: tuning profiles first broadened (leading to similar neural responses for different sensory stimuli) before tuning width recovered and many more AI neurons responded strongly to paired stimuli (facilitating detection and recognition of target tones). Changes in narrowband task performance were prevented by infusion of AP5 into locus coeruleus (Supplementary Fig. 12c, d, open circles).

The duration of these changes induced by a single episode of locus coeruleus pairing was considerably longer-lasting than behavioral changes induced by nucleus basalis pairing (Supplementary Fig. 13). Single episodes of nucleus basalis pairing produced improvements in detection (Supplementary Fig. 13a–c) and recognition (Supplementary Fig. 13d–f) that lasted several hours<sup>35</sup> but not longer. Instead, lasting improvements with nucleus basalis pairing required multiple episodes of pairing over several days, in contrast to the rapid and enduring behavioral changes produced by a single session of locus coeruleus pairing.

In our last experiment we asked whether locus coeruleus pairing might also accelerate reversal learning. Animals were first trained to respond to 4 kHz tones, before the rewarded tone was switched to 16 kHz (and 4 kHz became a foil). We monitored animals for several weeks after this reversal of reward contingency. The day of reversal, some animals received a single episode of locus coeruleus pairing with 16 kHz. Unpaired animals required 20+ days to recover initial performance levels, but paired animals learned the new association in almost half the time (Fig. 8f, g). Consequentially, locus coeruleus pairing improves perceptual abilities for at least hours after pairing, and even longer-lasting gains in performance can emerge over days to weeks after just a single pairing episode. These abilities can be enhanced beyond gains induced by reward-based training alone.

## Discussion

The locus coeruleus is the principal source of noradrenergic modulation for the central nervous system, providing a basic mechanism for adapting cortical circuits to task demands. Previous studies found that locus coeruleus neurons in rodents and primates respond to sensory stimuli after conditioning<sup>36,37</sup>. Here we showed that enduring contextual associations can be rapidly formed within the locus coeruleus, and cells previously unresponsive to sounds could become tonally responsive. The rapid induction and prolonged duration of these changes is reminiscent of changes to brain state and behavior in cases of one-trial learning or post-traumatic stress disorder<sup>38</sup>, suggesting that locus coeruleus plasticity is a fundamental determinant of these memory processes.

Locus coeruleus plasticity depends on NMDA receptors within the locus and can be induced by pairing tones with depolarization of single neurons. This form of long-term synaptic plasticity is likely due to direct modifications of excitatory transmission of connections into or within locus coeruleus. Given the short latency of these auditory responses from stimulus onset and the speed at which acoustic information can reach AI (~10 msec), we suspect that auditory inputs from frontal cortex and/or amygdala become sensitized after pairing<sup>26–28</sup>. Interestingly, blockade of locus coeruleus plasticity with AP5 was observed in animals anesthetized with ketamine, indicating that ketamine at these doses does not completely antagonize NMDA receptors, or that the anesthetic action of ketamine in the locus coeruleus is independent of NMDA receptors.

Locus coeruleus plasticity exerts a profound effect on downstream modulatory targets, controlling dynamics of cortical plasticity and auditory perceptual learning from induction to long-term maintenance. Noradrenergic modulation seems to provide a specific disinhibitory signal to cortical circuits, transiently reducing spontaneous inhibition in a similar manner as in dorsal cochlear nucleus<sup>24</sup>. This form of modulatory control is distinct from that provided by cholinergic modulation from nucleus basalis. Although both modulators reduce GABAergic inhibition in the cortex, acetylcholine downregulates stimulus-evoked inhibition<sup>17,35</sup> while noradrenalin reduces tonic inhibition. There may be an anatomical basis for this distinction depending on the projection patterns of cholinergic vs. noradrenergic axons, synaptic vs. extrasynaptic localization of receptor subtypes, and other factors governing the spatial and temporal scales of neuromodulation<sup>39–41</sup>, but there are limited data on any of these important issues.

Moreover, the physiological and behavioral changes induced by a single episode of nucleus basalis pairing are smaller and briefer as changes triggered by locus coeruleus pairing. The powerful disinhibitory effects of locus coeruleus stimulation on inhibitory tone might naturally lead to stronger and longer-lasting forms of cortical modifications, especially if NMDA receptor activation and postsynaptic spike generation are increased. Indeed, our results demonstrate that even a short amount of locus coeruleus pairing is sufficient to induce tone-evoked responses in previously-unresponsive neurons and convert subthreshold responses into spiking responses, similar to a recent study of spike-timing-dependent plasticity in rat visual cortex<sup>42</sup>. We hypothesize that the prolonged duration of locus coeruleus plasticity is also due to longer-term changes induced within locus coeruleus after pairing.

Effects of locus coeruleus pairing and cortical noradrenergic modulation are also distinct from dopamine, another catecholamine transmitter and the monoamine precursor for noradrenergic biosynthesis. Dopamine is released by the ventral tegmental area (VTA), and pairing VTA stimulation with pure tones produces a stimulus-specific and timing-dependent form of plasticity in rat AI<sup>43</sup>. Similarly, pairing a conditioned auditory stimulus with reward has similar effects on tonotopic map organization as VTA pairing<sup>44</sup>, consonant with the hypothesis that dopamine neurons are activated by appetitive reinforcement or reward prediction errors<sup>45,46</sup>. VTA stimulation can also enhance learning rates and peak performance on auditory tasks<sup>47</sup>. However, these changes are likely mechanistically distinct from the action of norepinephrine. While the predominant feature of noradrenergic

modulation in AI is reduction of tonic inhibition, dopaminergic modulation has a wide variety of effects including regulation of cAMP levels, enhancement of NMDA receptor signaling, and decreases of spontaneous spiking<sup>48,49</sup>.

Taken together, these data indicate that separate neuromodulatory systems can differentially control neural circuits by a variety of mechanisms, providing a high level of control over excitability, synaptic transmission, plasticity, and cognition. Norepinephrine in particular seems to control overall gain of cortical neurons, transiently increasing the effective salience of any incoming signal before cortical representations are more selectively refined. Importantly, this suggests that the functional organization of cortical receptive fields might be highly state-dependent. For example, in a low-arousal state when locus coeruleus firing rates are low, cortical neurons may be tuned to one stimulus, but during heightened states of arousal when locus coeruleus firing rates increase, cortical tuning curves might rapidly shift to prefer a different stimulus that previously occurred in conjunction with locus coeruleus activation. In support of this hypothesis, we found that when cortical alpha-noradrenergic receptors were blocked after locus coeruleus pairing, shifts in AI tuning curves induced by pairing were not apparent. Instead, cortical neurons resumed their original pre-pairing tuning preferences, although the mechanisms by which the original tuning preference is restored remain unclear.

Although these changes initially impair some aspects of sensory perception, lasting behavioral enhancements emerge over a period of hours to weeks, even after one pairing episode. The time course and dynamics of AI modifications are strikingly similar to the behavioral consequences of locus coeruleus pairing on detection and recognition of a rewarded pure tone stimulus. Additionally, locus coeruleus pairing also accelerated the progression of reversal learning, after the rewarded tone was changed from an unpaired tone to the tone that was paired with locus coeruleus stimulation. Although we have not yet identified the mechanisms that enhance reversal learning, it is possible that an extensive set of changes must occur to reconfigure the AI network and other brain areas involved in this behavior. Specifically, changes induced by locus coeruleus pairing (at a stimulus that was previously a non-target but then became the new target) are at odds with the learned association between reward and stimulus (specifically the tone that was the original target frequency). The reversal of reward contingency likely recruits a number of neuromodulatory systems, including the cholinergic nucleus basalis and dopaminergic VTA, leading to multiple forms or a composite form of plasticity enabled by cortical neuromodulation. Consequentially, for several days following reversal, cortical responses would appear much more 'confused' and complex than in highly-trained animals. However, the changes triggered by locus coeruleus pairing might provide some latent support for the reorganizations required to learn new associations, ultimately manifesting as an acceleration of the reversal process.

The full neural circuit representing learned associations between external stimuli and internal state is likely to be distributed throughout much of the brain, especially because neuromodulatory systems have extensive recurrent connections<sup>28</sup>. Under natural conditions, many of these systems might be engaged and co-regulated for control of cortical responses

and brain state, and modifications to neuromodulator systems provides a powerful mechanism for storing and restoring the most behaviorally-important memories.

## Online Methods

### Surgical preparation

All procedures were approved under NYU Institutional Animal Care and Use Committee protocols, in animals kept in a vivarium on a 12/12 hour light/dark cycle and housed individually or in pairs. Experiments were carried out in a sound-attenuating chamber. Female Sprague-Dawley rats 3–5 months old were anesthetized with ketamine (1.2 ml/kg) and dexmedetomidine (1.0 ml/kg), or pentobarbital (50 mg/kg). A bipolar stimulation electrode was implanted in the right locus coeruleus using stereotaxic coordinates (from lambda, in mm: 3.6 posterior, 1.2 lateral, 5.6–6 ventral). Location was verified during procedures by measuring responses to noxious stimuli (tail pinch, Supplementary Fig. 1a) and other electrophysiological criteria (spontaneous rates, Supplementary Fig. 1d), and afterwards using histological methods (Supplementary Fig. 1c, e). However, as our study involved making multiple recordings from the same location within the same animals, it was not always possible to resolve which specific recordings came from which cells. A craniotomy was performed over the right temporal lobe and the right auditory cortex was exposed. Pure tones (10–80 dB SPL, 0.5–32 kHz, 50 msec, 3 msec cosine on/offramps) were delivered in pseudo-random sequence at 0.5–1 Hz. Initial studies were performed at 0.5 Hz stimulation rate, but later experiments were performed at 1 Hz rates as there was no significant difference in the amount of plasticity induced at these two frequencies ( $P=0.1$ ). AI location was determined by mapping multiunit responses 500–700  $\mu\text{m}$  below the surface using tungsten electrodes. For infusion of drugs to the locus coeruleus, a hybrid cannula/stimulation electrode was used (Plastics One). For some recordings in locus coeruleus, a hemi-cerebellectomy was performed using gentle suction<sup>33</sup>, to expose the pons, allowing access of both an extracellular bipolar stimulation electrode (at a 30° angle) and a whole-cell recording pipette (at vertical orientation) to locus coeruleus.

Animals were perfused with 4% paraformaldehyde, brains recovered, and embedded in Optimal Cutting Temperature compound prior to freezing at  $-80^{\circ}\text{C}$ . Afterwards, 40  $\mu\text{m}$  thick slices were cut from the brainstem and stained using standard immunohistochemistry histological methods. Staining for tyrosine hydroxylase (primary antibody 1:1000, Aves Labs catalog number TYH; secondary antibody, DYL488 anti-chicken, 1:500, Life Technologies Labs) was co-localized with either biocytin staining revealed with Alexa Fluor 555 conjugated Streptavidin (1:100, Life Technologies Labs) or YFP (Abcam catalog number ab290).

### Electrophysiology

*In vivo* whole-cell recordings from locus coeruleus or AI neurons were made with a Multiclamp 700B amplifier (Molecular Devices). For current-clamp recordings, patch pipettes (5–9 M $\Omega$ ) contained (in mM): 135 K-gluconate, 5 NaCl, 5 MgATP, 0.3 GTP, 10 phosphocreatine, 10 HEPES, pH 7.3. For voltage-clamp recordings, pipettes contained: 125 Cs-gluconate, 5 TEACl, 4 MgATP, 0.3 GTP, 10 phosphocreatine, 10 HEPES, 0.5 EGTA,

3.5 QX-314, 2 CsCl, pH 7.2. In some cases, 1% biocytin (Sigma) was added to the internal solution for post-hoc recovery of recorded neurons. Resting potential of locus coeruleus neurons:  $-62.4 \pm 12.5$  mV (s.d.); series resistance (Rs):  $31.6 \pm 11.0$  M $\Omega$ ; input resistance (Ri):  $214.5 \pm 131.8$  M $\Omega$ . Whole-cell recordings from locus coeruleus neurons were obtained using two different methods, depending on the manner of postsynaptic stimulation during pairing. For single cell stimulation, recordings were obtained 5500–6000  $\mu$ m from the pial surface. During pairing, cells were depolarized through the patch pipette (20 Hz for 500 msec). For extracellular stimulation, the cerebellum was aspirated and recordings were obtained  $\sim$ 300  $\mu$ m below the surface of the pons.

Recordings from AI neurons were obtained from cells located 400–1200  $\mu$ m below the pial surface. Resting potential of AI neurons:  $-63.0 \pm 10.8$  mV; Rs:  $23.0 \pm 12.7$  M $\Omega$ ; Ri:  $109.8 \pm 55.4$  M $\Omega$ . Data were excluded if Rs changed  $>30\%$  or Ri changed  $>50\%$  from values measured during baseline. Data were filtered at 5 kHz, digitized at 20 kHz, and analyzed with Clampfit 10 (Molecular Devices). For locus coeruleus pairing, after recording baseline responses to the pseudo-random tone sequence for each cell for 5–20 minutes, a non-preferred tone of a given intensity level and frequency was repetitively presented for 1–5 min (at least one minute, no more than five minutes, and generally ceased if large changes to responses were observed in between), concurrent with locus coeruleus stimulation (500 msec, 20 Hz, 0.01 msec pulse duration, 20 V stimulation strength) starting at tone onset. Afterwards, locus coeruleus stimulation was ceased and pseudo-random tone sequences were resumed. For nucleus basalis stimulation experiments of Supplementary Figure 8, animals had bipolar stimulation electrodes implanted in nucleus basalis (stereotaxic coordinates from bregma, in mm: 2.3 posterior, 3.3 lateral, 7 ventral) instead of locus coeruleus. Nucleus basalis stimulation during pairing was at 100 Hz for 250 msec, in the same manner as our previous studies<sup>17,35</sup>.

For analysis of tonal responses in locus coeruleus neurons in Figure 1f, we computed z-scores from mean peak EPSPs 20–50 msec after tone onset post-pairing, compared to the mean and standard deviation of responses during this same period before pairing. For analysis of tuning curve shifts in Figures 2–4, 6 and 7, best frequency shift was computed as the normalized difference in octaves between the paired frequency and the original best frequency, such that if the best frequency became the paired frequency, this was a 100% shift, whereas if the best frequency stayed the same, this was a 0% shift. To determine tuning curve width, Gaussians were fit to tuning profiles, and the changes in standard deviation measured in terms of number of octaves. For determining post-pairing changes in evoked activity in Figure 5, we compared the average response during the baseline period to the average response 6–10 minutes post-pairing. Spontaneous events were automatically detected using a template, and changes to spontaneous rates and amplitudes were also compared pre-pairing and 6–10 minutes post-pairing.

For AP5 infusions in Figures 1 and 7, in some experiments we used custom hybrid cannula/stimulation electrodes implanted into locus coeruleus, and AP5 was infused (0.1–1 mM in saline, 1  $\mu$ l total volume at 0.2  $\mu$ l/min). In other experiments in which a hemi-cerebellectomy was performed, AP5 (0.1–1 mM) was topically applied to locus coeruleus. Results of AP5 application at higher (1 mM) and lower (0.1 mM) concentrations were similar ( $p > 0.7$ ) and

so results were combined. For norepinephrine iontophoresis in Figure 6a, double-barreled iontophoresis pipettes (20–30 M $\Omega$ ) contained norepinephrine (0.1 mM) in one barrel and saline in the other barrel; for bicuculline iontophoresis experiments of Supplementary Figure 11, one barrel contained bicuculline methiodide (1 mM) and the other barrel contained saline. Iontophoresis electrodes were placed 700  $\mu$ m below the pial surface, roughly 250–300  $\mu$ m from the recording pipette; retaining current was –10 nA and ejection current was +40 nA. For experiments of Figure 6b, c, phentolamine (0.1–1 mM in saline) was topically applied to AI. Results of phentolamine application at higher (1 mM) and lower (0.1 mM) concentrations were similar ( $P=0.3$ ) and so results were combined. These concentrations were used to ensure that many neurons in the locus coeruleus or cortex would be affected by pharmacological treatment, but it is important to note that especially near site of application, there may be non-specific effects on excitability or other transmitter systems.

For foot shock experiments of Supplementary Figures 1 and 2, a silver wire was connected to the hindlimb footpad. Foot shock (20–100 Hz, 500 msec duration, 40–150 V) was applied for 2–5 minutes.

To determine the effective activation radius of locus coeruleus stimulation in Supplementary Figure 1f, local field potentials (LFPs) were recorded with a tungsten electrode (0.5–1 M $\Omega$ ) lowered to 5500–6000  $\mu$ m below the cerebellar surface. Several penetrations were made at different distances from the stimulation electrode (100–2000  $\mu$ m). LFPs were digitized at 20 kHz and bandpass filtered between 1–100 Hz.

Stereotaxic viral injections were performed in TH-Cre Long-Evans rats. Animals were anesthetized with ketamine/dexmedetomidine, placed into a stereotaxic apparatus, and a craniotomy performed over locus coeruleus. Location was verified by measuring responses to tail pinch with a tungsten electrode, and then injections were performed with a 5  $\mu$ L Hamilton syringe and a 33 gauge needle. Cre-inducible pAAV5-EF1 $\alpha$ :-DIO-ChETA-EYFP virus<sup>50</sup> was injected into locus coeruleus at 0.1 nl/s for a final injection volume of 1.2–1.5  $\mu$ L. The virus was given a minimum of two weeks to express, and then a second craniotomy performed in the same location, and position was re-verified by recording responses to tail pinch. A calibrated optical fiber ferrule was then implanted in locus coeruleus, and the craniotomy and implant was sealed with dental cement. For optogenetic stimulation in TH-Cre rats expressing the ChETA variant of channelrhodopsin-2, a non-preferred tone of a given intensity level and frequency was repetitively presented for 1–5 min, concurrent with optical stimulation of locus coeruleus (500 msec, 20 Hz, 0.01 msec pulse duration, 1–3 mW) starting at tone onset.

Unless otherwise noted, all statistics and error bars are reported as means $\pm$ s.e.m. although normality was not formally tested for all data sets, and p-values determined from Student's paired or unpaired two-tailed t-tests. Multiple comparisons were not necessary unless otherwise noted, and studies were not analyzed blind to the conditions of the experiments. No statistical methods were used to predetermine sample sizes for electrophysiological experiments, as our sample sizes are similar to or larger than what is standard in the field. Electrophysiological experiments were not randomized in terms of which cells were paired under different conditions.

## Behavior

Rats were lightly food-deprived and pre-trained for 2–6 weeks on a frequency recognition go/no-go task<sup>35</sup>. Animals were rewarded with food for nose-poking within three seconds of presentation of a target tone (4 kHz, any intensity), and given a short (~5 s) time out if they incorrectly responded to non-target tones. After learning to nosepoke to 4 kHz tones, spectrally-wideband foils were also presented (0.5, 1, 2, 8, 16, 32 kHz). Animals that achieved hit rates >80% for targets were then anesthetized with ketamine/dexmedetomidine, had stimulation electrodes or hybrid cannula/stimulation electrodes chronically implanted in right locus coeruleus, and were allowed to recover for a week before being randomly assigned to an experimental group for further study. Sixteen other animals had electrodes implanted in nucleus basalis instead. Animals were generally tested during the light cycle, but sometimes were tested during the dark cycle as well for measuring the extended time course of behavioral changes. Animals that did not achieve >80% hit rates with 6 weeks or had damaged implants were excluded from further analysis.

Each implanted animal was first tested on the ‘wideband’ recognition task or the detection task for at least 1–2 days. On the wideband and narrowband recognition tasks, tones (wideband target: 4 kHz, foils: 0.5, 1, 2, 8, 16, 32 kHz; narrowband target: 4 kHz, foils: 2.8, 3.2, 3.6, 4.5, 5.1, 5.7 kHz) were presented at 70 dB SPL. For the detection task, tones were presented at 20–90 dB SPL. On the first day at each task, tones were presented for 30–60 minutes to assess performance at baseline; 4 kHz tones (at 70 dB SPL for the wideband recognition task; 30–45 dB SPL for the detection task; hits binned over 20–40 dB SPL) were then paired with locus coeruleus stimulation in the training box for two to three minutes, and behavior performance assessed and quantified one, three, twelve and/or twenty four hours after one single episode of stimulation. In some cases, animal performance was monitored over the span of weeks, once a day, to examine the duration of behavioral changes induced by locus coeruleus pairing. For reversal learning, 17 Sprague-Dawley rats and eight Long-Evans rats (four wild-type, four *TH-Cre*) had the rewarded tone switched from 4 kHz to 16 kHz on the wideband task after achieving  $d' > 2.0$ . Six of those animals had stimulation electrodes implanted in locus coeruleus and three *TH-Cre* animals had fiber optics implanted in locus coeruleus, and electrical or optical locus coeruleus stimulation was paired with 16 kHz tones for five minutes just prior to testing behavioral performance on the first day that 16 kHz was rewarded. Performance was measured daily thereafter. Cannulated animals had AP5 (1 mM in saline, 0.4–1  $\mu$ l at 0.2 $\mu$ l/min) or saline infused into the locus coeruleus immediately prior to stimulation for either task.  $d'$  values were computed as the difference in z-scores between hits and false positives:  $d' = z(\text{hit rate}) - z(\text{false positive rate})$ , using the responses between 20–40 dB SPL for detection and responses to 3.6–4.5 kHz for narrowband recognition. Unless otherwise noted, all statistics and error bars are reported as means $\pm$ s.e.m. although normality was not formally tested for all data sets, and p-values determined from Student’s paired or unpaired two-tailed t-tests. Power analysis was performed to determine the number of animals required for statistical significance as in our previous study of the same behaviors in rats<sup>35</sup>. For detection performance after locus coeruleus pairing, effect size was 1.48 and power was 0.99, requiring at least three animals; for detection performance after nucleus basalis pairing over multiple days, effect size was 1.10 and power was 0.82, requiring at least three animals. For recognition performance after

locus coeruleus pairing, effect size was 0.67 and power was 0.80, requiring at least 12 animals; for recognition performance after nucleus basalis pairing over multiple days, effect size was 2.03 and power was 0.97, requiring at least two animals. Studies were not performed blind to the conditions of the experiments.

A supplementary methods checklist is available.

## Supplementary Material

Refer to Web version on PubMed Central for supplementary material.

## Acknowledgments

We thank I. Carcea, C. Clopath, A.M. Gomez, M. Jin, J.E. LeDoux, M.A. Long, L.J. Miller, C.N. Parkhurst, D.B. Polley, S.D. Shea, I. Shehu, and N. Zaika for comments, discussions, and technical assistance, and C.A. Loomis and the NYU School of Medicine Histology Core for assistance with anatomical studies. J. Pivkova created artwork in Fig. 1a and Fig. 2a; S.E. Ross created artwork in Supplementary Fig. 12a. This work was funded by NIDCD (DC009635 and DC012557), a Hirschl/Weill-Caulier Career Research Award and a Sloan Research Fellowship (R.C.F.), and the Portuguese Foundation for Science and Technology (A.R.O.M).

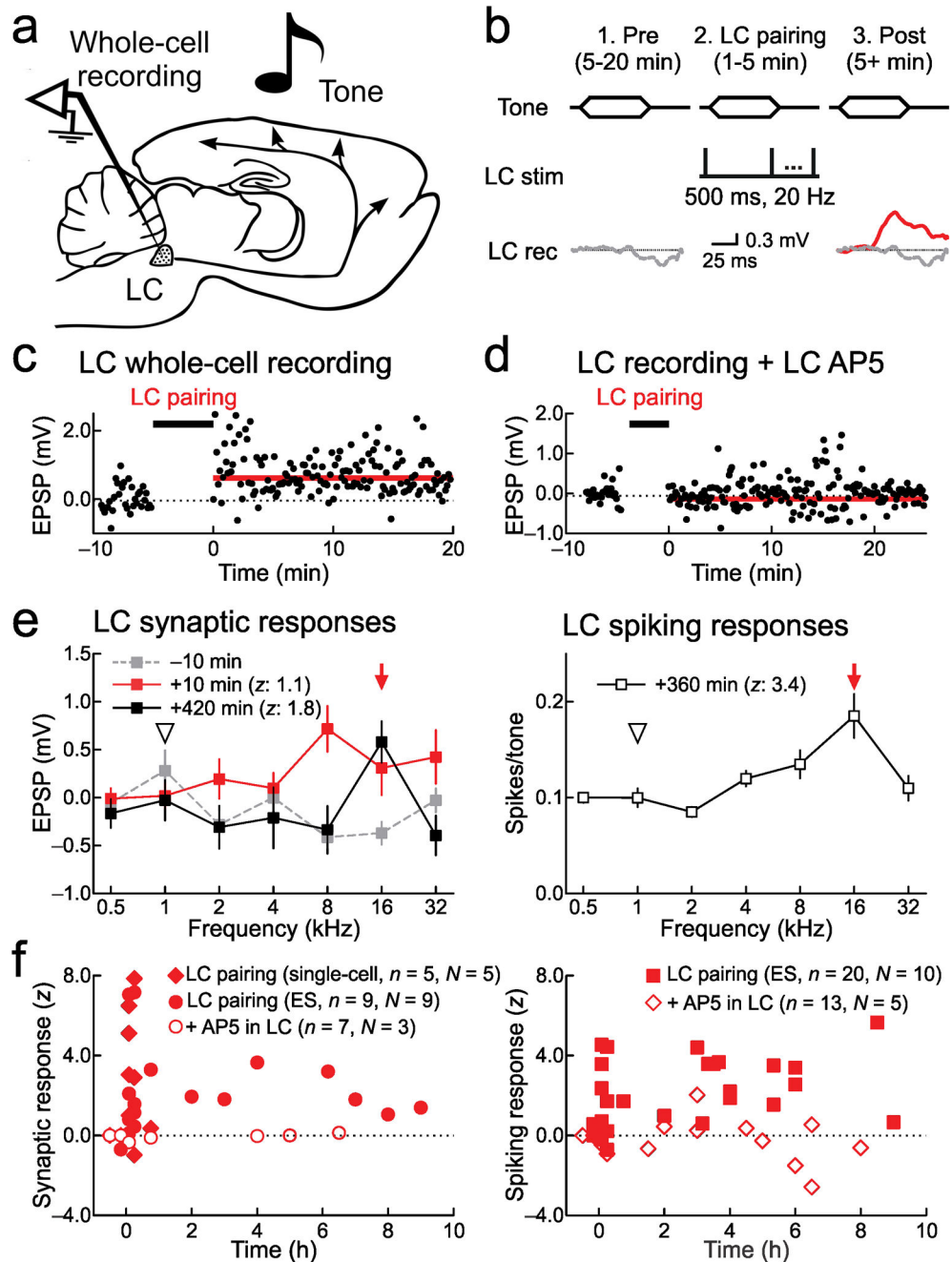
## References

1. Katz LC, Shatz CJ. Synaptic activity and the construction of cortical circuits. *Science*. 1996; 274:1133–1138. [PubMed: 8895456]
2. Hensch TK. Critical period regulation. *Annu Rev Neurosci*. 2004; 27:549–579. [PubMed: 15217343]
3. Feldman DE, Brecht M. Map plasticity in somatosensory cortex. *Science*. 2005; 310:810–815. [PubMed: 16272113]
4. Gilbert CD, Li W, Piech V. Perceptual learning and adult cortical plasticity. *J Physiol*. 2009; 587:2743–2751. [PubMed: 19525560]
5. Levelt CN, Hübener M. Critical-period plasticity in the visual cortex. *Annu Rev Neurosci*. 2012; 35:309–330. [PubMed: 22462544]
6. Znamenskiy P, Zador AM. Corticostriatal neurons in auditory cortex drive decisions during auditory discrimination. *Nature*. 2013; 497:482–485. [PubMed: 23636333]
7. Buonomano DV, Merzenich MM. Cortical plasticity: from synapses to maps. *Annu Rev Neurosci*. 1998; 21:149–186. [PubMed: 9530495]
8. Fritz J, et al. Rapid task-related plasticity of spectrotemporal receptive fields in primary auditory cortex. *Nat Neurosci*. 2003; 6:1216–1223. [PubMed: 14583754]
9. Ohl FW, Scheich H. Learning-induced plasticity in animal and human auditory cortex. *Curr Opin Neurobiol*. 2005; 15:470–477. [PubMed: 16009546]
10. Froemke RC, Martins ARO. Spectrotemporal dynamics of auditory cortical synaptic receptive field plasticity. *Hear Res*. 2011; 279:149–161. [PubMed: 21426927]
11. Sanes DH, Woolley SM. A behavioral framework to guide research on central auditory development and plasticity. *Neuron*. 2011; 72:912–929. [PubMed: 22196328]
12. Marlin BJ, Mitre M, D'Amour JA, Chao MV, Froemke RC. Oxytocin enables maternal behavior by balancing cortical inhibition. *Nature*. 2015; 520:499–504. [PubMed: 25874674]
13. Bakin JS, Weinberger NM. Induction of a physiological memory in the cerebral cortex by stimulation of the nucleus basalis. *Proc Natl Acad Sci U S A*. 1996; 93:11219–11224. [PubMed: 8855336]
14. Marder E. From biophysics to models of network function. *Annu Rev Neurosci*. 1998; 21:25–45. [PubMed: 9530490]
15. Shulz DE, et al. A neuronal analogue of state-dependent learning. *Nature*. 2000; 403:549–553. [PubMed: 10676963]



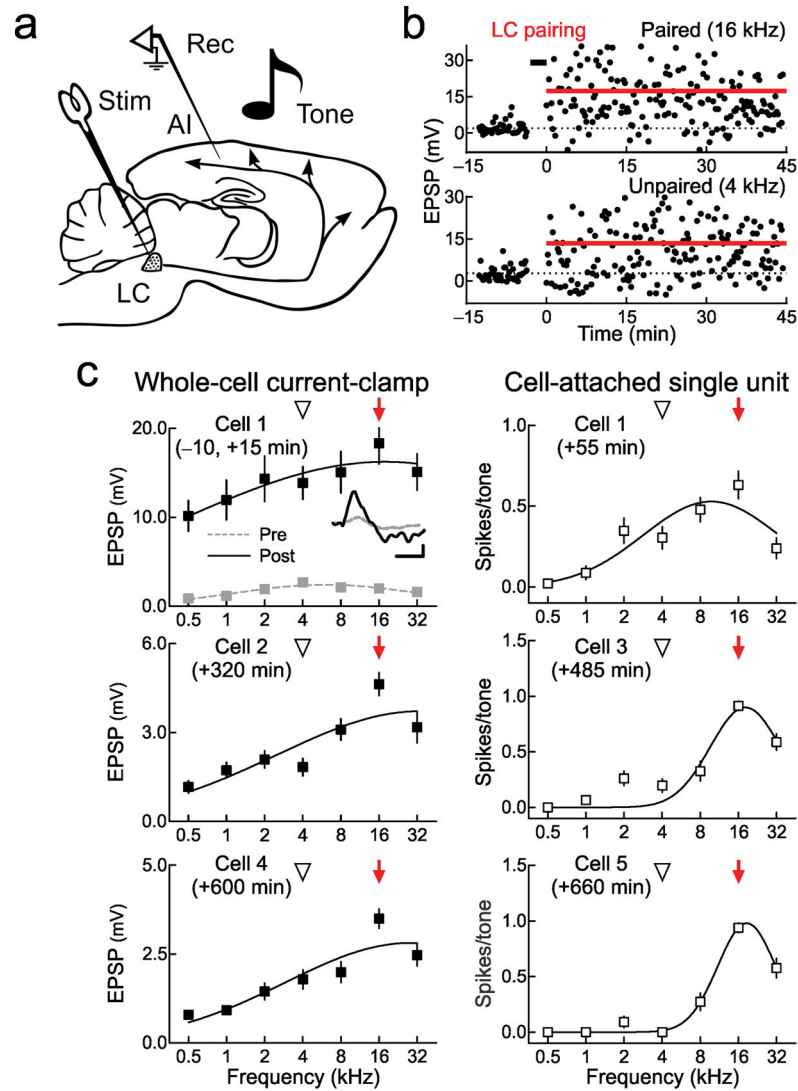
16. Gu Q. Neuromodulatory transmitter systems in the cortex and their role in cortical plasticity. *Neuroscience*. 2002; 111:815–835. [PubMed: 12031406]
17. Froemke RC, et al. A synaptic memory trace for cortical receptive field plasticity. *Nature*. 2007; 450:425–429. [PubMed: 18004384]
18. Constantinople CM, Bruno RM. Effects and mechanisms of wakefulness on local cortical networks. *Neuron*. 2011; 69:1061–1068. [PubMed: 21435553]
19. Chun S, et al. Thalamocortical long-term potentiation becomes gated after the early critical period in the auditory cortex. *J Neurosci*. 2013; 33:7345–7357. [PubMed: 23616541]
20. Bear MF, Singer W. Modulation of visual cortical plasticity by acetylcholine and noradrenaline. *Nature*. 1986; 320:172–176. [PubMed: 3005879]
21. Hu H, et al. Emotion enhances learning via norepinephrine regulation of AMPA-receptor trafficking. *Cell*. 2007; 131:160–173. [PubMed: 17923095]
22. Bush DE, et al. Beta-adrenergic receptors in the lateral nucleus of the amygdala contribute to the acquisition but not the consolidation of auditory fear conditioning. *Front Behav Neurosci*. 2010; 4:154. [PubMed: 21152344]
23. Edeline JM, et al. Induction of selective plasticity in the frequency tuning of auditory cortex and auditory thalamus neurons by locus coeruleus stimulation. *Hear Res*. 2011; 274:75–84. [PubMed: 20709165]
24. Kuo SP, Trussell LO. Spontaneous spiking and synaptic depression underlie noradrenergic control of feed-forward inhibition. *Neuron*. 2011; 71:306–318. [PubMed: 21791289]
25. Eldar E, et al. The effects of neural gain on attention and learning. *Nat Neurosci*. 2013; 16:1146–1153. [PubMed: 23770566]
26. Aston-Jones G, Cohen JD. An integrative theory of locus coeruleus-norepinephrine function: adaptive gain and optimal performance. *Annu Rev Neurosci*. 2005; 28:403–450. [PubMed: 16022602]
27. Berridge CW. Noradrenergic modulation of arousal. *Brain Res Rev*. 2008; 58:1–17. [PubMed: 18199483]
28. Sara SJ. The locus coeruleus and noradrenergic modulation of cognition. *Nat Rev Neurosci*. 2009; 10:211–223. [PubMed: 19190638]
29. Carter ME, et al. Tuning arousal with optogenetic modulation of locus coeruleus neurons. *Nat Neurosci*. 2010; 13:1526–1533. [PubMed: 21037585]
30. Aston-Jones G, et al. Locus coeruleus neurons are selectively activated by attended cues in a vigilance task. *J Neurosci*. 1994; 14:4467–4480. [PubMed: 8027789]
31. Usher M, et al. The role of locus coeruleus in the regulation of cognitive performance. *Science*. 1999; 283:549–554. [PubMed: 9915705]
32. Yu AJ, Dayan P. Uncertainty, neuromodulation, and attention. *Neuron*. 2005; 46:681–692. [PubMed: 15944135]
33. Sugiyama D, et al. In vivo patch-clamp recording from locus coeruleus neurones in the rat brainstem. *J Physiol*. 2012; 590:2225–2231. [PubMed: 22371480]
34. Devilbiss DM, Waterhouse BD. Phasic and tonic patterns of locus coeruleus output differentially modulate sensory network function in the awake rat. *J Neurophysiol*. 2011; 105:69–87. [PubMed: 20980542]
35. Froemke RC, et al. Long-term modification of cortical synapses improves sensory perception. *Nat Neurosci*. 2013; 16:79–88. [PubMed: 23178974]
36. Sara SJ, Segal M. Plasticity of sensory responses of locus coeruleus neurons in the behaving rat: implications for cognition. *Prog Brain Res*. 1991; 88:571–585. [PubMed: 1813935]
37. Aston-Jones G, Rajkowski J, Kubiak P, Alexinsky T. Locus coeruleus neurons in monkey are selectively activated by attended cues in a vigilance task. *J Neurosci*. 1994; 14:4467–4480. [PubMed: 8027789]
38. Johansen JP, et al. Molecular mechanisms of fear learning and memory. *Cell*. 2011; 147:509–524. [PubMed: 22036561]
39. Disney AA, Reynolds JH. Expression of m1-type muscarinic acetylcholine receptors by parvalbumin-immunoreactive neurons in the primary visual cortex: a comparative study of rat,

- guinea pig, ferret, macaque, and human. *J Comp Neurol.* 2014; 522:986–1003. [PubMed: 23983014]
40. Muñoz W, Rudy B. Spatiotemporal specificity in cholinergic control of neocortical function. *Curr Opin Neurobiol.* 2014; 26:149–160. [PubMed: 24637201]
41. Froemke RC. Plasticity of cortical excitatory-inhibitory balance. *Annu Rev Neurosci.* 2015; 38:195–219. [PubMed: 25897875]
42. Pawlak V, Greenberg DS, Sprekeler H, Gerstner W, Kerr JN. Changing the responses of cortical neurons from sub- to suprathreshold using single spikes in vivo. *eLife.* 2013; 2:e00012. [PubMed: 23359858]
43. Bao S, Chan VT, Merzenich MM. Cortical remodelling induced by activity of ventral tegmental dopamine neurons. *Nature.* 2001; 412:79–83. [PubMed: 11452310]
44. Bieszczad KM, Weinberger NM. Representational gain in cortical area underlies increase of memory strength. *Proc Natl Acad Sci U S A.* 2010; 107:3793–3798. [PubMed: 20133679]
45. Schultz W, Dayan P, Montague PR. A neural substrate of prediction and reward. *Science.* 275:1593–1599. [PubMed: 9054347]
46. Bromberg-Martin ES, Matsumoto M, Hikosaka O. Distinct tonic and phasic anticipatory activity in lateral habenula and dopamine neurons. *Neuron.* 2010; 67:144–155. [PubMed: 20624598]
47. Shumake J, Ilango A, Scheich H, Wetzel W, Ohl FW. Differential neuromodulation of acquisition and retrieval of avoidance learning by the lateral habenula and ventral tegmental area. *J Neurosci.* 2010; 30:5876–5883. [PubMed: 20427648]
48. Seamans JK, Yang CR. The principal features and mechanisms of dopamine modulation in the prefrontal cortex. *Prog Neurobiol.* 2004; 74:1–58. [PubMed: 15381316]
49. Huang Y, Mylius J, Scheich H, Brosch M. Tonic effects of the dopaminergic ventral midbrain on the auditory cortex of awake macaque monkeys. *Brain Struct Funct.* 2014 in press.
50. Gunaydin LA, et al. Ultrafast optogenetic control. *Nat Neurosci.* 2010; 13:387–392. [PubMed: 20081849]

**Figure 1.**

Locus coeruleus responses are plastic. **a**, In vivo whole-cell or cell-attached recording from locus coeruleus (“LC”) neurons. **b**, Locus coeruleus pairing procedure. Scale: 0.3 mV, 25 msec. **c**, Current-clamp recording from locus coeruleus neuron. Dotted line, baseline tone-evoked EPSP ( $0.0 \pm 0.1$  mV). Red line, tone-evoked EPSP after pairing ( $0.7 \pm 0.1$  mV,  $P = 10^{-8}$ , Student’s unpaired two-tailed t-test; z-score: 3.0). **d**, Recording with AP5 infusion (1 mM); no response to tones before ( $0.0 \pm 0.1$  mV) or after pairing ( $-0.1 \pm 0.1$  mV,  $P = 0.3$ ; z-score:  $-0.3$ ). **e**, Three locus coeruleus neurons for 7+ hours before and after pairing. Left,

first recording ten minutes before (gray; tone-evoked EPSPs:  $-0.4 \pm 0.1$  mV) and ten minutes post-pairing (red; tone-evoked EPSPs:  $0.3 \pm 0.3$  mV,  $P=0.004$ , z-score: 1.1); third recording 420 minutes post-pairing (black; tone-evoked EPSPs:  $0.6 \pm 0.2$  mV, z-score: 1.8). Right, second cell-attached recording 360 minutes post-pairing ( $0.2 \pm 0.02$  spikes/tone; z-score: 3.4). **f**, Summary of new tonal responses in locus coeruleus neurons after pairing. Left, synaptic responses (33 measurements,  $n=14$  neurons,  $N=9$  animals; z-score 5–15 minutes post-pairing:  $3.1 \pm 0.8$ ,  $P=0.0009$ ; z-score 3–10 hours post-pairing:  $2.0 \pm 0.5$ ,  $P=0.02$ ). Filled diamonds, experiments pairing with single-cell depolarization instead of extracellular stimulation ('ES'). Open symbols, AP5 in locus coeruleus ( $n=7$ ,  $N=3$ ; z-score 5–15 minutes post-pairing:  $-0.2 \pm 0.1$ ,  $P=0.3$ ; z-score 3–10 hours post-pairing:  $0.04 \pm 0.05$ ,  $P=0.4$ ). Right, spiking (35 measurements, 20 neurons, 10 animals; z-score 5–15 minutes post-pairing:  $1.6 \pm 0.6$ ,  $P=0.02$ ; z-score 3–10 hours post-pairing:  $2.9 \pm 0.4$ ,  $P=10^{-4}$ ; AP5,  $n=13$ ,  $N=5$ ; z-score 5–15 minutes post-pairing:  $-0.7 \pm 0.2$ ,  $P=0.2$ ; z-score 3–10 hours post-pairing:  $-1.0 \pm 0.7$ ,  $P=0.2$ ). Error bars indicate s.e.m.

**Figure 2.**

AI plasticity induced by locus coeruleus pairing with electrical stimulation. **a**, Setup: stimulation electrode (“Stim”) in locus coeruleus (“LC”) and recordings (“Rec”) from AI neurons. **b**, Current-clamp recording of responses to paired 16 kHz and unpaired 4 kHz tones. **c**, Synaptic (top) and spiking (bottom) tuning curves from five neurons before and 0–11 hours post-pairing from current-clamp (filled) or cell-attached recordings (open). Each recording from same AI location. Upper left, first recording ten minutes before (gray) and fifteen minutes after (black) pairing with 16 kHz. After pairing, best frequency shifted to 16 kHz (100% shift) and tuning width increased from 2.4 octaves to 5.3 octaves (221% width). EPSPs increased across frequencies (paired 16 kHz EPSPs:  $2.0 \pm 0.4$  mV pre-pairing,  $18.3 \pm 2.3$  mV post-pairing,  $P=10^{-8}$ ; unpaired EPSPs across other frequencies:  $1.7 \pm 0.3$  mV pre-pairing,  $13.4 \pm 0.8$  mV post-pairing,  $P=10^{-5}$ ). Same cell as **b**. Inset, 16 kHz EPSPs before (gray) and after (black) pairing; scale: 6 mV, 25 msec. Upper right, cell-attached recording 55 minutes post-pairing (best frequency shift: 100%, tuning curve width: 1.8 octaves). Middle left, second recording 320 minutes post-pairing (shift: 100%, width: 3.8 octaves).

Middle right, third recording 485 minutes post-pairing (shift: 100%, width: 0.9 octaves).  
Lower left, fourth recording 600 minutes post-pairing (shift: 100%, width: 3.3 octaves).  
Lower right, fifth recording 660 minutes post-pairing (shift: 100%, width: 0.8 octaves).  
Error bars indicate s.e.m.

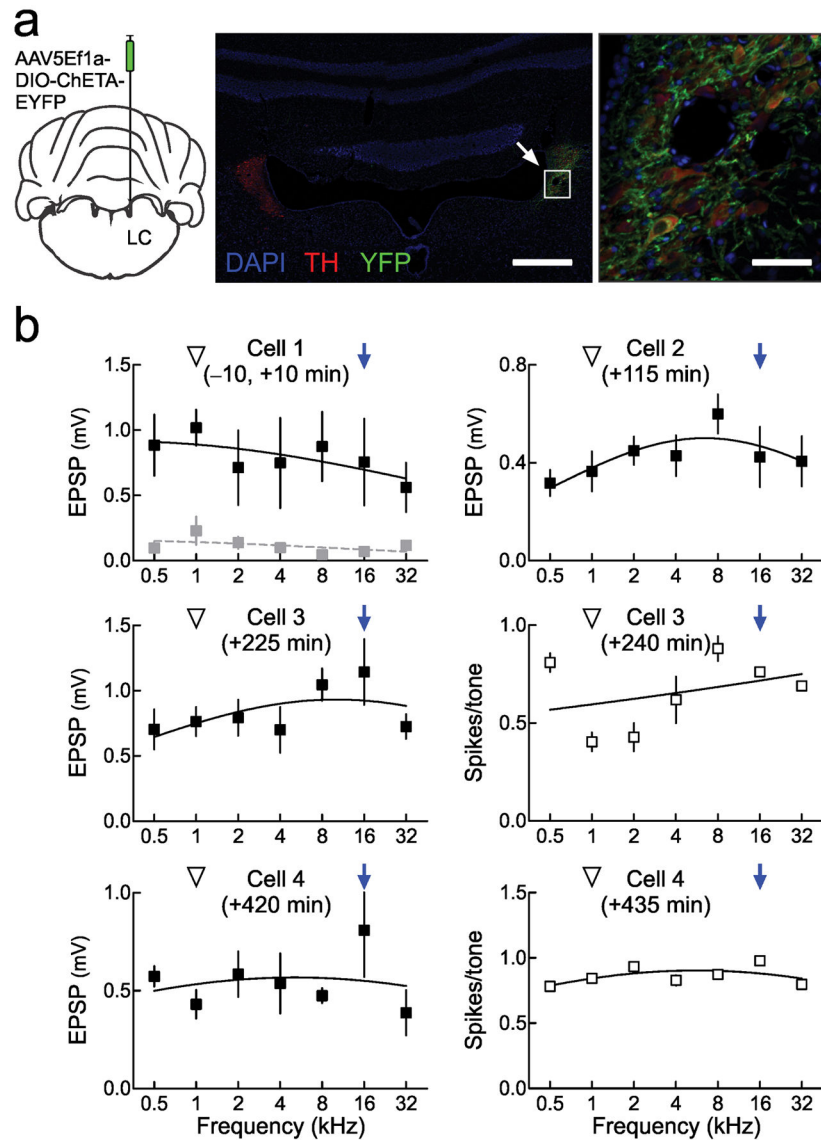


**Figure 3.**

AI plasticity induced by locus coeruleus pairing with optical stimulation in *TH-Cre* rats. **a**, Optogenetic control of locus coeruleus. Left, schematic of viral injection. Animals had an AAV expressing the ChETA variant of channelrhodopsin-2 and YFP (AAV5Efla-DIO ChETA-EYFP) stereotaxically injected into right locus coeruleus. Middle, TH and YFP immunostaining in locus coeruleus imaged at 10X; red, TH; green, YFP; blue, DAPI. Tissue was examined this way in one animal. Arrow, injection site. Scale, 500  $\mu$ m. Right, zoom-in of white boxed region in middle panel showing co-labeling of TH and YFP expression. Scale, 40  $\mu$ m. **b**, Synaptic and spiking tuning curves from four neurons before and 0–7 hours post-pairing from current-clamp (filled) or cell-attached recordings (open). Each recording from same AI location. Upper left, first recording ten minutes before (gray) and ten minutes after (black) pairing optical stimulation with 16 kHz (arrow). EPSPs increased across frequencies (paired 16 kHz EPSPs:  $0.1 \pm 0.05$  mV pre-pairing,  $0.8 \pm 0.2$  mV post-pairing,

$P=0.001$ ; unpaired EPSPs across other frequencies:  $0.1\pm 0.02$  mV pre-pairing,  $0.9\pm 0.06$  mV post-pairing,  $P=10^{-15}$ ). Upper right, second cell-attached recording 115 minutes post-pairing (best frequency shift: 75%). Middle left, third recording 225 minutes post-pairing (shift: 100%). Middle right, third recording 240 minutes post-pairing (shift: 75%). Lower left, fourth recording 420 minutes post-pairing (shift: 100%). Lower right, fourth recording 435 minutes post-pairing (shift: 100%). Error bars indicate s.e.m.

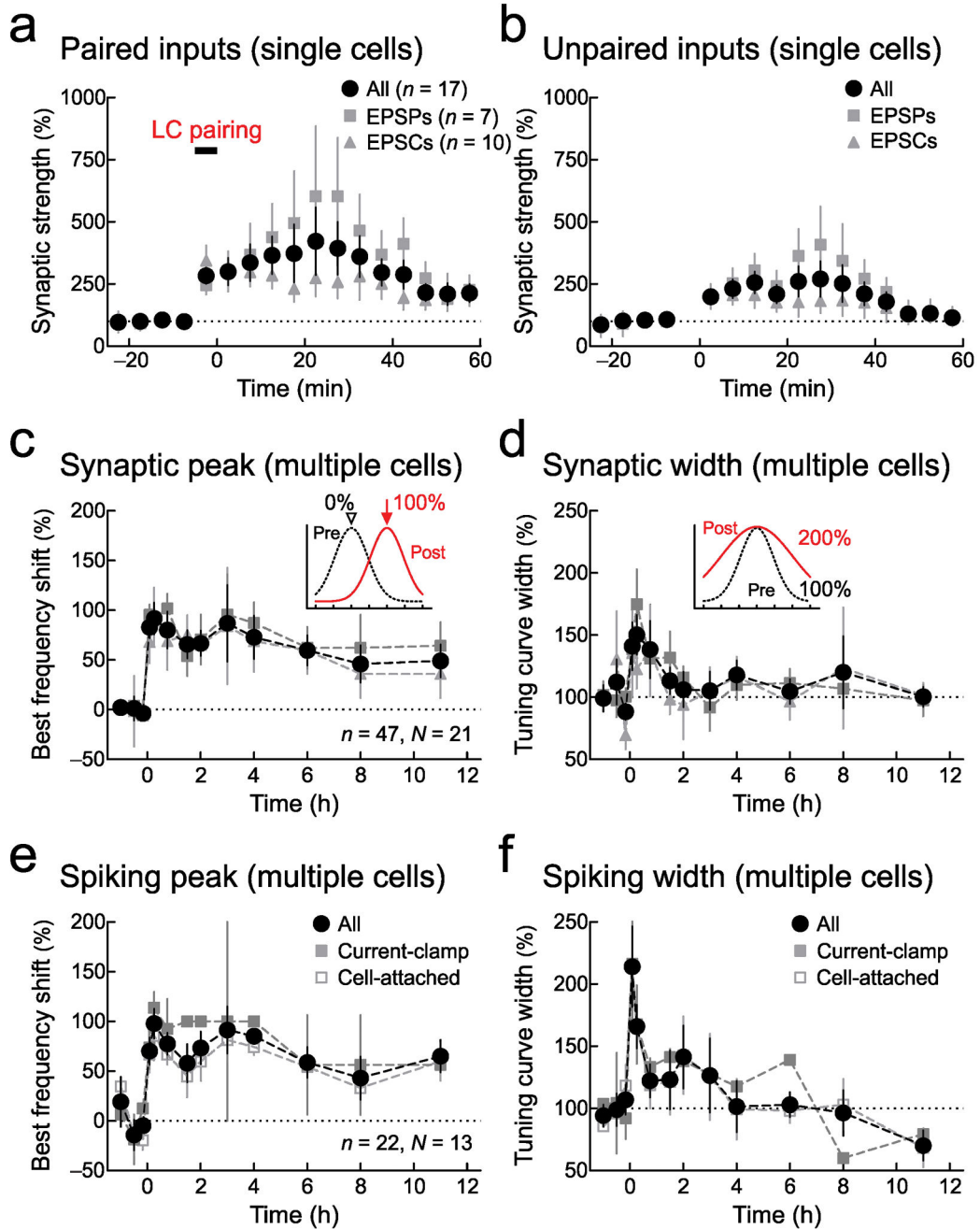
Author Manuscript

Author Manuscript

Author Manuscript

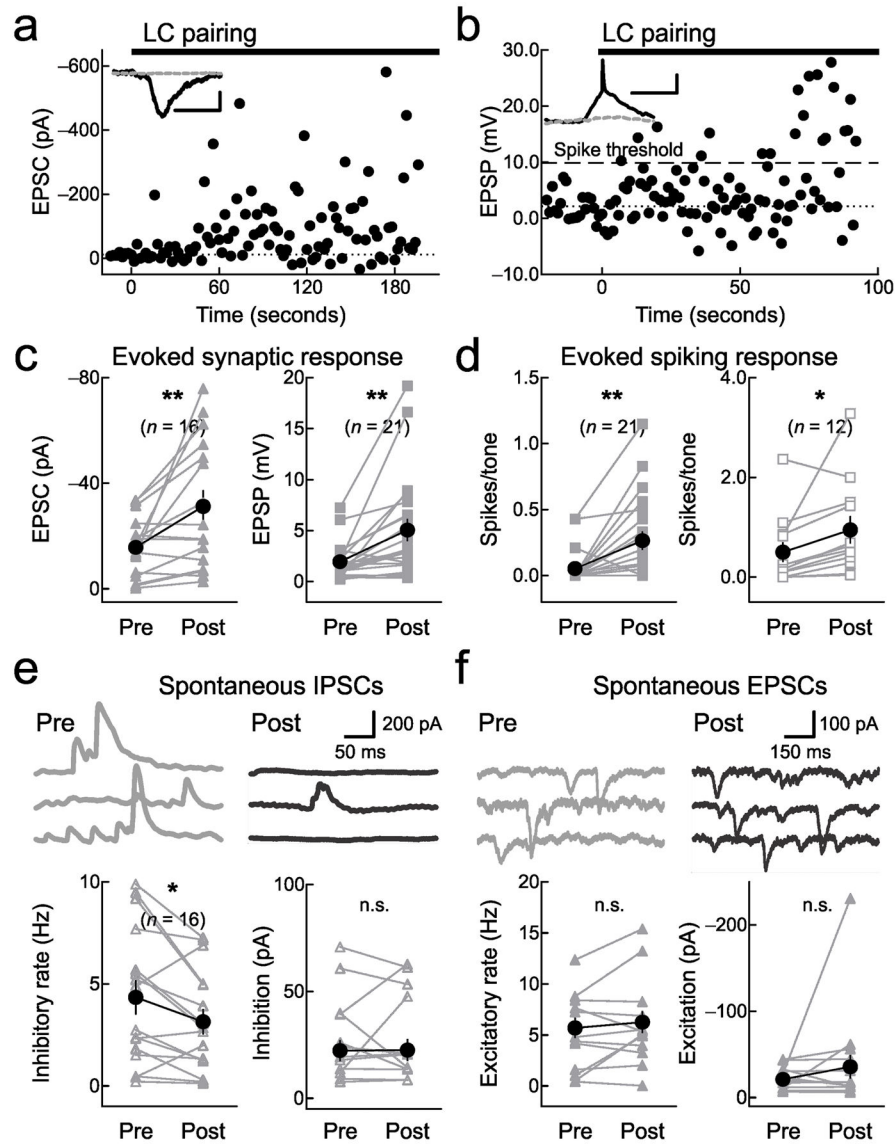
Author Manuscript



**Figure 4.**

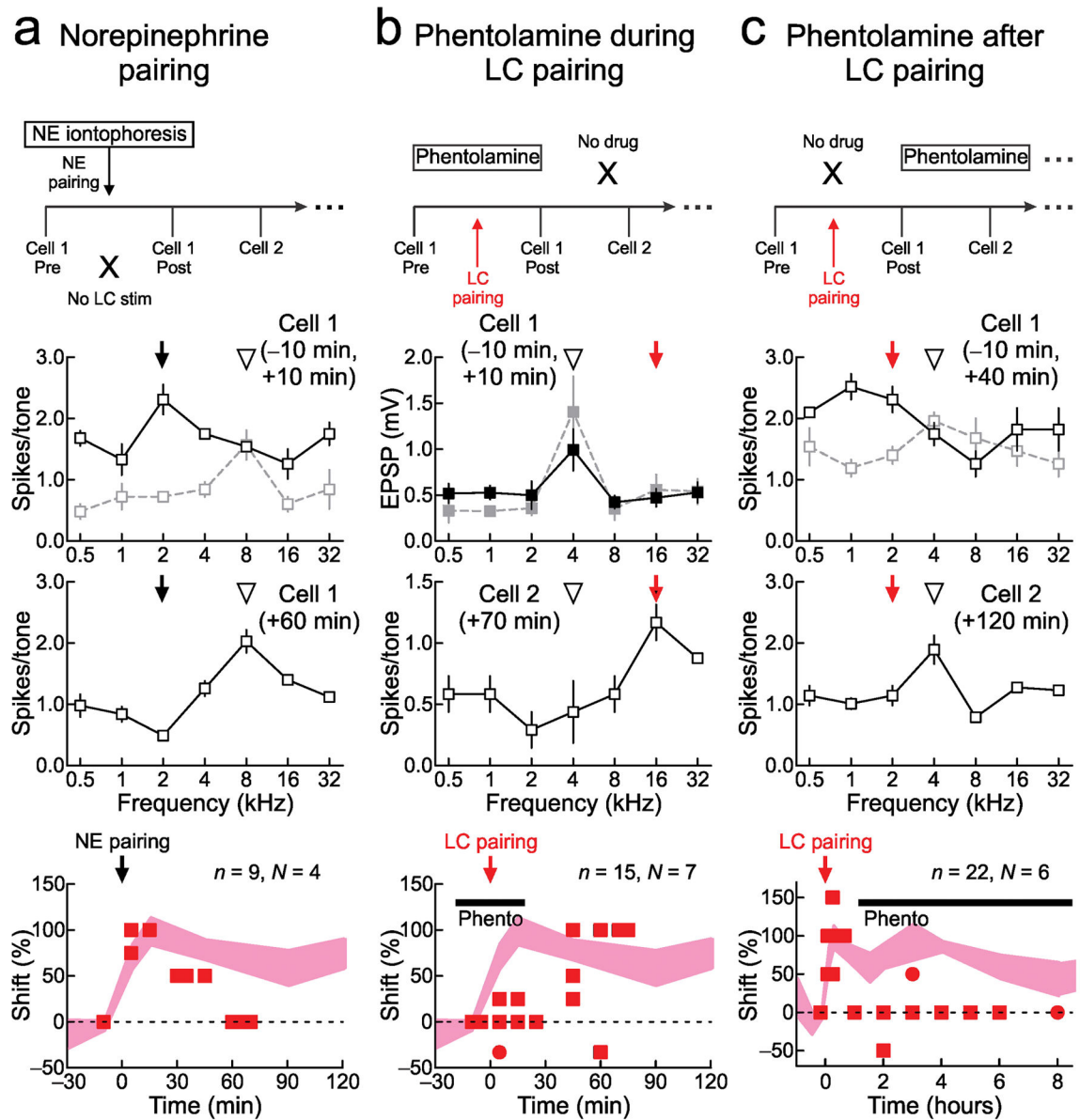
Changes to synaptic and spiking tuning curves after locus coeruleus pairing. **a**, Changes to paired inputs from individual recordings. Circles, all recordings (5–10 minutes:  $335.9 \pm 74.8\%$ ,  $n=37$  neurons,  $P=0.0003$ ; 45–60 minutes:  $261.2 \pm 62.8\%$ ,  $n=17$ ,  $P=0.01$ ); squares, current-clamp ( $n=21$ ); triangles, voltage-clamp ( $n=16$ ). **b**, Changes to unpaired inputs from individual recordings for all recordings (5–10 minutes:  $231.1 \pm 38.3\%$ ,  $P=0.03$ ; 45–60 minutes:  $151.0 \pm 49.4\%$ ,  $P=0.2$ ). **c**, Best frequency shift of synaptic tuning over multiple recordings (circles,  $n=87$  neurons,  $N=37$  animals; 5–30 minutes:  $90.6 \pm 10.7\%$ ,

$P=10^{-9}$ ; 7–12 hours:  $65.6\pm 12.5\%$ ,  $n=27$ ,  $N=13$ ,  $p<P=0.0002$ ; squares, current-clamp,  $n=47$ ; triangles, voltage-clamp,  $n=40$ ). **d**, Synaptic tuning curve width over multiple recordings (5–30 minutes:  $146.6\pm 14.8\%$ ,  $n=37$ ,  $N=37$ ,  $P=10^{-40}$ .; 7–12 hours:  $103.3\pm 7.8\%$ ,  $n=27$ ,  $N=13$ ,  $P=0.1$ ). Same recordings as **c**. **e**, Best frequency shifts of spiking tuning curves over multiple recordings (circles,  $n=72$ ,  $N=34$ ; 5–30 minutes:  $89.7\pm 11.4\%$ ,  $n=29$ ,  $N=29$ ,  $P=10^{-5}$ ; 7–12 hours:  $66.1\pm 11.5\%$ ,  $n=21$ ,  $N=11$ ,  $P=0.002$ ; filled squares, current-clamp,  $n=22$ ; open squares, cell-attached,  $n=50$ ). **f**, Widening of spiking tuning curves over multiple recordings (5–30 minutes:  $188.5\pm 15.1\%$ ,  $n=29$ ,  $N=29$ ,  $P=0.001$ ; 7–12 hours:  $93.6\pm 11.5\%$ ,  $n=21$ ,  $N=11$ ,  $P=0.7$ ). Same recordings as **e**. All comparisons with Student's paired two-tailed t-tests. Error bars indicate s.e.m.

**Figure 5.**

Cortical circuit mechanisms of enhanced AI responses after locus coeruleus pairing. **a**, Voltage-clamp recording showing new tone-evoked responses during pairing. Inset, responses before (gray), during pairing (black); scale: 150 pA, 10 msec. **b**, Current-clamp recording showing sub- to suprathreshold tone-evoked responses. Dashed line, spike threshold. Scale: 5 mV, 10 msec. **c**, Synaptic changes. Left, voltage-clamp recordings (pre:  $-15.7 \pm 2.8$  pA, post:  $-31.3 \pm 6.2$  pA;  $n = 16$ ,  $P = 0.006$ ). 10/16 recordings had significant tone-evoked responses before pairing, 14/16 post-pairing ( $P < 0.05$  for each cell). Right, current-clamp recordings (pre:  $2.0 \pm 0.4$  mV, post:  $5.1 \pm 1.1$  mV;  $n = 21$ ,  $P = 0.002$ ). 18/21 recordings had significant tone-evoked responses before pairing, 20/21 post-pairing. **d**, Spiking changes. Left, current-clamp recordings (pre:  $0.05 \pm 0.03$  spikes/tonne, post:  $0.25 \pm 0.07$  spikes/tonne;  $n = 21$ ,  $P = 0.004$ ). 4/21 recordings had 1+ tone-evoked spikes before pairing, 13/21 post-pairing. Right, cell-attached recordings (pre:  $0.5 \pm 0.2$  spikes/tonne, post:  $0.9 \pm 0.3$  spikes/tonne;

$n=12$ ,  $P=0.04$ ). 9/12 recordings had 1+ tone-evoked spikes before pairing, 12/12 post-pairing. **e**, Spontaneous IPSCs. Top, pairing decreased spontaneous IPSC rate (pre: 9.2 Hz, post: 5.0 Hz) but not amplitude (pre: 70.8 pA, post: 61.3 pA). Left, IPSC rate (pre:  $4.3 \pm 0.8$  Hz, post:  $3.1 \pm 0.6$  Hz;  $n=16$ ,  $P=0.01$ ). Right, amplitude (pre:  $24.6 \pm 4.7$  pA, post:  $24.7 \pm 4.9$  pA;  $n=16$ ,  $P=0.9$ ). 'n.s.', non-significant. **f**, Spontaneous EPSCs. Top, pairing did not affect spontaneous EPSC rate (pre: 12.4 Hz, post: 15.4 Hz) or amplitude (pre: -44.3 pA, post: -56.7 pA). Same recording as **e**. Left, EPSC rate (pre:  $5.7 \pm 1.0$  Hz, post:  $6.3 \pm 1.1$  Hz;  $n=16$ ,  $P=0.3$ ). Right, amplitude (pre:  $-21.1 \pm 3.0$  pA, post:  $-35.7 \pm 13.7$  pA;  $n=16$ ,  $P=0.2$ ). All comparisons with Student's paired two-tailed t-tests. Error bars indicate s.e.m.

**Figure 6.**

Noradrenergic receptor activation is required for expression of AI plasticity. **a**, Norepinephrine pairing ('NE pairing') leads to shorter-term but not sustained AI changes. Top, experimental design; pure tones were paired with NE iontophoresis (0.1 mM) in AI. Middle, cell-attached recording before and after NE pairing with 2 kHz (arrow). Initially, best frequency (open arrowhead) shifted from 8 kHz to 2 kHz, but returned to 8 kHz one hour later. Bottom, NE pairing summary (best frequency shift 10 minutes post-pairing:  $95.8 \pm 5.1\%$ ,  $n=4$ ,  $N=4$ ,  $P=10^{-5}$ ; shift 45+ minutes post-pairing:  $8.3 \pm 10.2\%$ ,  $n=4$ ,  $N=4$  animals,  $P=0.3$ ). **b**, Cortical phentolamine (0.1–1 mM) only during LC pairing prevents shorter-term changes, but longer-term changes emerge when phentolamine is removed. Top, experimental design. Middle, whole-cell recording before and after pairing, and cell-attached recording one hour post-pairing. Original best frequency was 4 kHz, tuning was

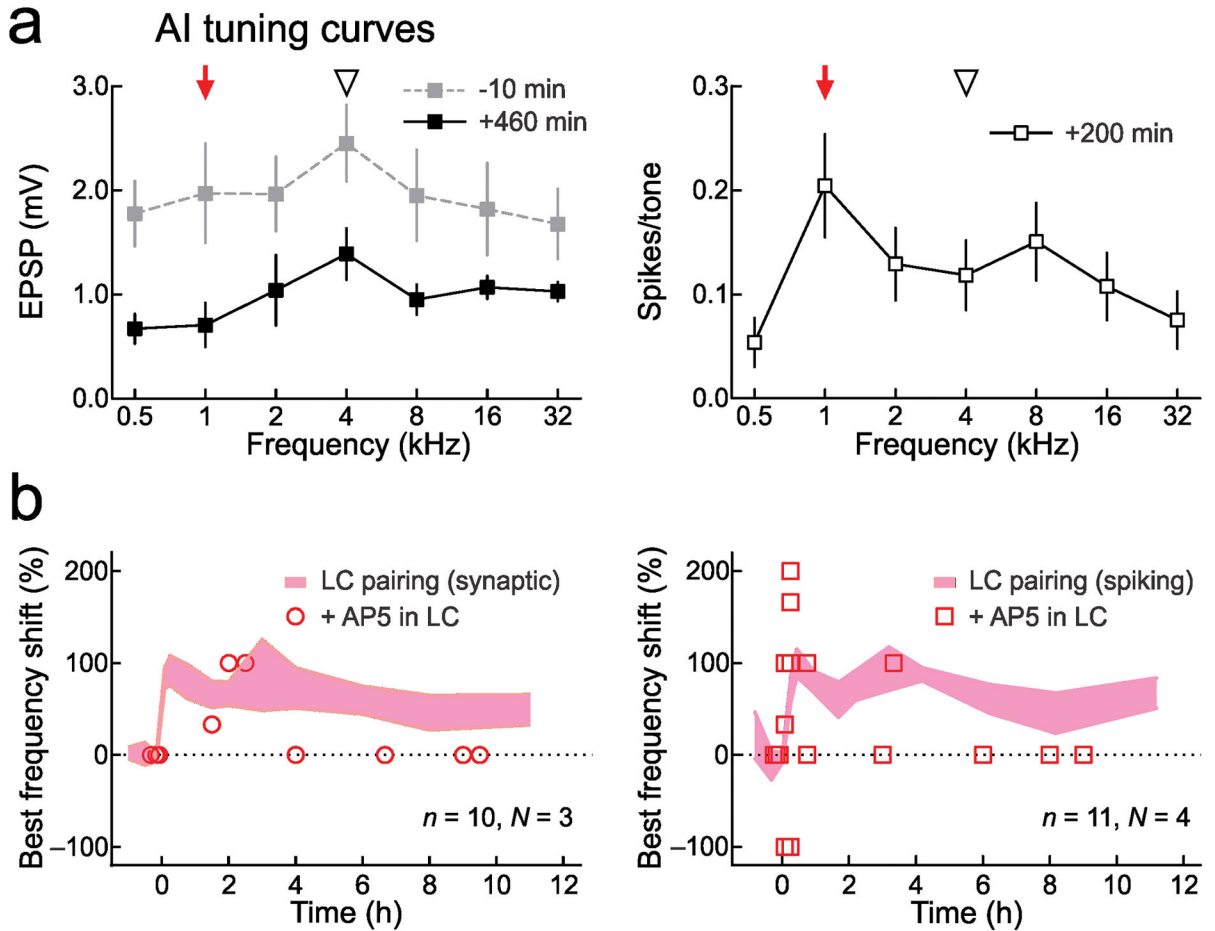
unchanged 10 minutes post-pairing in presence of phentolamine (0.1 mM), but shifted to paired 16 kHz tone one hour later when phentolamine was removed. Bottom, phentolamine during pairing summary (shift 10 minutes post-pairing:  $1.5 \pm 62\%$ ,  $n=6$ ,  $N=6$ ,  $P=0.7$ ; shift 45+ minutes post-pairing:  $67.8 \pm 17.7\%$ ,  $n=8$ ,  $N=7$ ,  $P=0.0006$ ). c, Phentolamine applied after pairing for hours shortens AI shift duration. Top, experimental design-phentolamine (0.1 mM) was applied to AI for subsequent recordings after pairing. Middle, two cell-attached recordings before and after LC pairing. Bottom, phentolamine after pairing summary (shift 10 minutes post-pairing:  $85.0 \pm 10.7\%$ ,  $n=6$ ,  $N=6$ ,  $P=10^{-4}$ ; shift 3–8 hours post-pairing:  $6.3 \pm 6.3\%$ ,  $n=8$ ,  $N=5$ ,  $P=0.3$ ). All comparisons with unpaired two-tailed t-tests. Error bars indicate s.e.m.

Author Manuscript

Author Manuscript

Author Manuscript

Author Manuscript

**Figure 7.**

Locus coeruleus plasticity controls the duration of cortical plasticity. **a**, Three AI recordings for 7+ hours pre/post-pairing with AP5 in locus coeruleus. Left, first current-clamp recording ten minutes before (gray) pairing; third current-clamp recording 460 minutes post-pairing (black). 4 kHz was original best frequency (arrowhead); 1 kHz was paired frequency (arrow). Right, second cell-attached recording 200 minutes post-pairing. **b**, Summary of AI best frequency shift with AP5 in locus coeruleus. Left, synaptic AI best frequency shift. After 2–10 hours post-pairing, best frequency returned to baseline (shift:  $33.3 \pm 21.1\%$ ,  $P=0.1$ ,  $n=6$  neurons,  $N=3$  animals). Shaded area, mean  $\pm$  s.e.m. of shifts from Figure 4c. Right, spiking best frequency shift (shift:  $20.0 \pm 20.0\%$ ,  $P=0.3$ ,  $n=5$ ,  $N=4$ ). Shaded area, mean  $\pm$  s.e.m. from Figure 4e. Error bars indicate s.e.m.

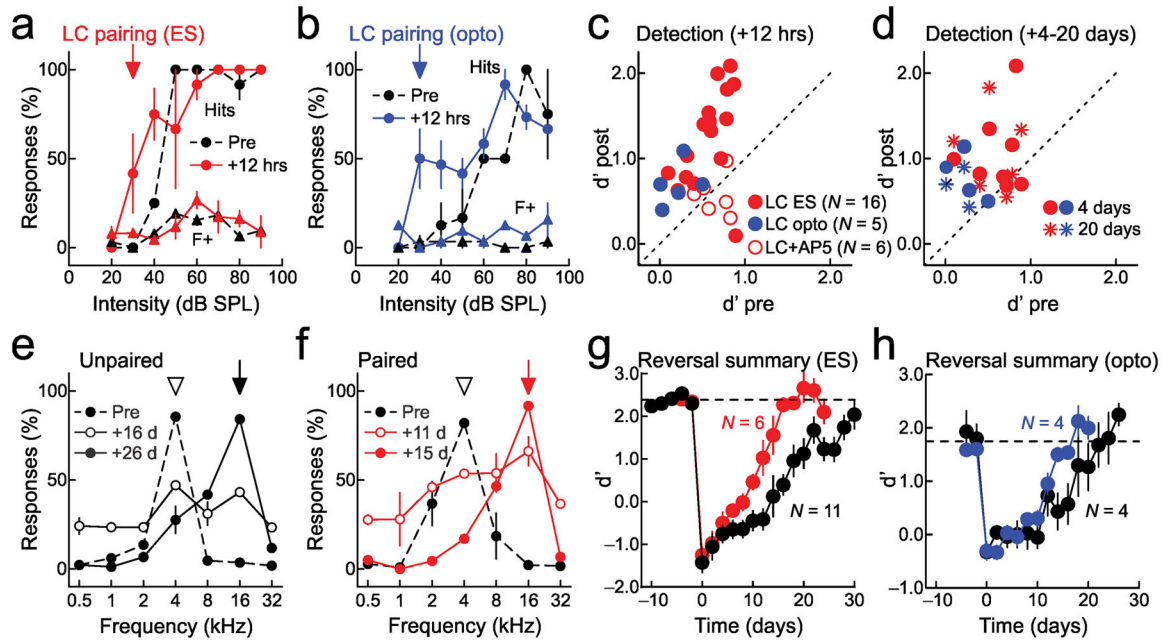


**Figure 8.**

Locus coeruleus pairing improves sensory perception. **a**, Enhanced detection after pairing 30 dB SPL, 4 kHz tones with electrical stimulation ('ES') of locus coeruleus. Hits (circles) at 20–40 dB SPL increased after 12 hours (pre-pairing, black:  $8.3 \pm 5.3\%$ , post-pairing, red:  $43.7 \pm 14.0\%$ ,  $P=0.04$ ); foil responses (triangles) were unchanged (pre-pairing:  $3.6 \pm 1.7\%$ , post-pairing:  $6.8 \pm 1.8\%$ ,  $P=0.2$ ), increasing  $d'$  (0.5 to 1.4). **b**, Enhanced detection after pairing 30 dB SPL, 4 kHz tones with optogenetic locus coeruleus stimulation ('opto'). Hits at 20–40 dB SPL increased after 12 hours (pre-pairing, black:  $5.0 \pm 5.0\%$ , post-pairing, blue:  $38.7 \pm 11.8\%$ ,  $P=0.04$ ); foils were unchanged (pre-pairing:  $2.7 \pm 1.6\%$ , post-pairing:  $3.8 \pm 2.5\%$ ,  $P=0.7$ ), increasing  $d'$  (0.3 to 1.1). **c**,  $d'$  values (before:  $0.49 \pm 0.06$ , 12 hours after:  $1.12 \pm 0.12$ ,  $N=21$ ,  $P=10^{-5}$ , Student's paired two-tailed t-test). AP5 in locus coeruleus prevented improvement (open circles;  $d'$  before:  $0.65 \pm 0.07$ , after:  $0.57 \pm 0.10$ ,  $N=6$ ,  $P=0.5$ ). **d**, Detection was enhanced four days (circles;  $d'$  before:  $0.49 \pm 0.09$ , after:  $0.98 \pm 0.12$ ,  $N=12$ ,  $P=0.004$ ) and 20 days after pairing (stars; before:  $0.44 \pm 0.09$ , after:  $0.89 \pm 0.14$ ,  $N=10$ ,  $P=0.01$ ). **e**, Reversal learning without pairing; rewarded frequency was changed to 16 kHz. **f**, One pairing episode (at 16 kHz) accelerated reversal learning. **g**, Accelerated reversal learning after electrical LC pairing. Sliding t-tests (width: two days) used to determine when performance recovered to baseline (black, control: 22 days,  $N=11$ ; red, paired animals: 13 days,  $N=6$ ). **h**, Accelerated reversal learning after optogenetic LC pairing. Performance recovered faster in paired animals (black, control: 17 days,  $N=4$ ; blue, paired animals: 13 days,  $N=4$ ). Error bars indicate s.e.m.